Chemically Stable Piperidinium Cations for Anion Exchange Membranes

Jinyuan Li [a,b,c], Congrong Yang [a,b], Suli Wang [a,b*], Zhangxun Xia [a,b] and Gongquan Sun [a,b*]

[a] *Division of Fuel Cells and Battery, Dalian National Laboratory for Clean Energy, Dalian Institute of Chemical Physics, Chinese Academy of Sciences, Dalian 116023, China*

[b] *Key Laboratory of Fuel Cells & Hybrid Power Sources, Chinese Academy of Sciences, Dalian 116023, China*

[c] *University of Chinese Academy of Sciences, Beijing 100039, China*

Corresponding Authors

*gqsun@dicp.ac.cn; suliwang@dicp.ac.cn

1. Synthesis of piperidinium cations

Synthesis of N,N-dimethylpiperidinium iodide ([MePip][I]): [MePip][I] was synthesized by stirring a mixture of N-methylpiperidine (7.90 g, 79.66 mmol) and methyl iodide (13.23 g, 93.21 mmol) at room temperature. Afterwards, the mixture was added to an excess of ethyl acetate to precipitate the target solid. Then, the powder was washed twice with ethyl acetate, collected and dried under vacuum and 80 ℃ to obtain [MePip][I]. White solid. ^{1}H NMR (400 MHz, D_2O, ppm, Figure S16a): δ 3.26-3.18 (H_a), δ 3.02 (H_d), δ 1.84-1.77 (H_b), δ 1.57 (H_c).

Synthesis of N-butyl-N-methylpiperidinium bromide ([BuPip][Br]): [BuPip][Br] was synthesized by stirring a mixture of N-methylpiperidine (7.90 g, 79.66 mmol) and 1-bromobutane (12.69 g, 92.61 mmol) at 80 ℃ for 2 h. Afterwards, the mixture was added to an excess of ethyl acetate to precipitate the target solid. Then, the powder was washed twice with ethyl acetate, collected and dried under vacuum and 80 ℃ to obtain [BuPip][Br]. Yellow solid. ^{1}H NMR (400 MHz, D_2O, ppm, Figure S16b): δ 3.24 (H_a, H_e), δ 2.93 (H_d), 1.79 (H_b), δ 1.63 (H_c, H_f), δ 1.31 (H_g), δ 0.87 (H_h).

Synthesis of N-hexyl-N-methylpiperidinium bromide ([HePip][Br]): [HePip][Br] was synthesized by stirring a mixture of N-methylpiperidine (1.95 g, 19.71 mmol) and 1-bromohexane (3.52 g, 21.34 mmol) at 80 ℃ for 5 h. Afterwards, the mixture was added to an excess of ethyl acetate to precipitate the target solid. Then, the powder was washed twice with ethyl acetate, collected and dried under vacuum and 80 ℃ to obtain [HePip][Br]. Orange-red solid. ^{1}H NMR (400 MHz, D_2O, ppm, Figure S16c): δ 3.23 (H_a, H_e), δ 2.93 (H_d), δ 1.79 (H_b), 1.71-1.51 (H_c, H_f), δ 1.34-1.20 (H_h, H_h, H_i), δ

0.79 (H_j).

Synthesis of N-isopropyl-N-methylpiperidinium iodide ([iPrPip][I]): [iPrPip][I] was synthesized by stirring a mixture of N-methylpiperidine (4.07 g, 41.06 mmol) and 2-iodopropane (8.17 g, 48.10 mmol) in chloroform (17 ml) at 60 ℃ for 8 h. After the evaporation of solvent, the mixture was added to an excess of ethyl acetate to precipitate the target solid. Then, the powder was washed twice with ethyl acetate, finally collected and dried under vacuum and 80 ℃ to obtain [iPrPip][I]. Yellow solid. ^{1}H NMR (400 MHz, D_2O, ppm, Figure S16d): δ 3.75 (H_e), δ 3.26 (H_a), δ 2.80 (H_d), δ 1.80 (H_b), 1.58 (H_c), δ 1.29 (H_f).

Synthesis of N-isobutyl-N-methylpiperidinium bromide ([iBuPip][Br]): [iBuPip][Br] was synthesized by stirring a mixture of N-methylpiperidine (7.90 g, 79.66 mmol) and 1-bromo-2-methylhexane (10.0 ml, 91.96 mmol) at 80 ℃ for 5 h. Afterwards, the mixture was added to an excess of ethyl acetate to precipitate the target solid. Then, the powder was washed twice with ethyl acetate, collected and dried under vacuum and 80 ℃ to obtain [iBuPip][Br]. Yellow solid. ^{1}H NMR (400 MHz, D_2O, ppm, Figure S16e): δ 3.28 (H_a), δ 3.15 (H_e), δ 2.99 (H_d), δ 2.18 (H_f), δ 1.81 (H_b), 1.59 (H_c), δ 1.05-0.99 (H_g).

2. Conductivity of SEBS-AEMs functionalized by trimethylammonium (SEBS-BTMA) and N-methylpiperidinium (SEBS-BzPip) in chloride form before and after treatment in alkaline condition

The stability of trimethylammonium and N-methylpiperidinium in AEMs was evaluated by analysis of the conductivity of home-made SEBS-based AEMs before and after exposure to alkaline conditions. The IEC value of both AEMs before stability test was about 1.2 mmol g^{-1}. Membranes were treated in 2 M KOH solution at 100 ℃ in a sealed Teflon container. After certain time periods, samples were taken out and the anions in the membranes were exchanged to Cl^- in 2 M NaCl solution. The Cl^- conductivity of membranes were measured in the fully hydrated state by electrochemical impedance spectroscopy at 80 ℃. The conductivity change during the test is shown in Table S1.

Table S1. Conductivity of SEBS-BTMA and SEBS-BzPip in chloride form at 80 ℃ before and after treatment in 2 M KOH at 100 ℃.

Time (h)	SEBS-BTMA		SEBS-BzPip	
	σ (mS cm^{-1})	σ / σ (0 h) (%)	σ (mS cm^{-1})	σ / σ (0 h) (%)
0	40	100	34	100
96	35.4	88.50	32.95	96.91
168	20.38	50.95	19.94	58.65
216	19.22	48.05	18.38	54.06

3. NMR spectra for $[BzPip]^+$, $[BTMA]^+$ and $[BzPyr]^+$ synthesized for stability studies

Note: all ^1H NMR spectra in this part were taken in D_2O and referenced to the residual solvent peak (H_2O) at 4.79 ppm.

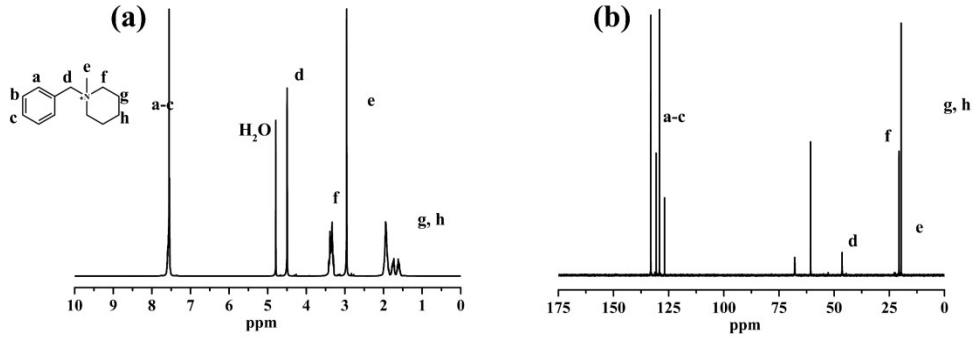

Figure S1. ^1H NMR (a) and ^{13}C NMR (b) spectra of $[BzPip]^+$ synthesized for stability study.

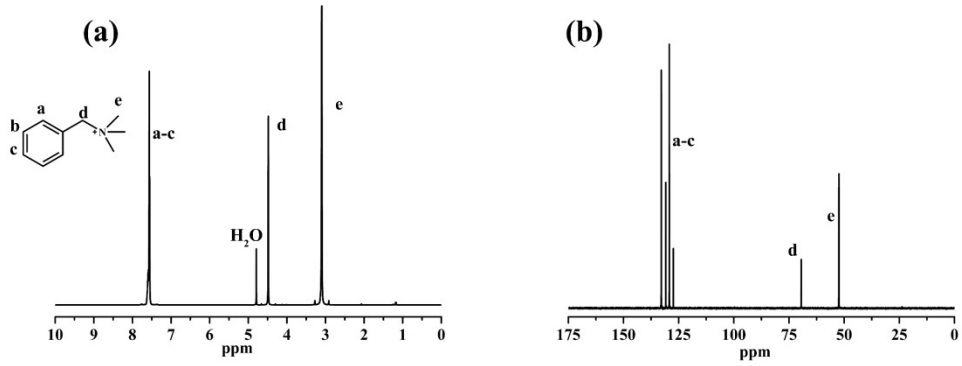

Figure S2. ^1H NMR (a) and ^{13}C NMR (b) spectra of $[BTMA]^+$ synthesized for stability study.

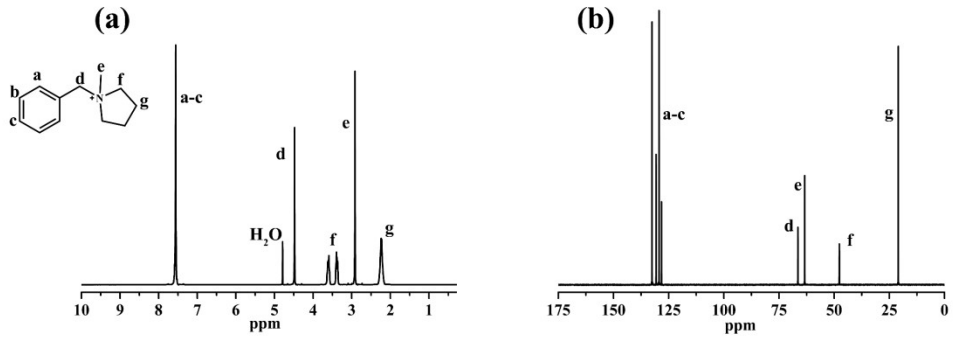

Figure S3. ^{1}H NMR (a) and ^{13}C NMR (b) spectra of $[BzPyr]^{+}$ synthesized for stability study.

4. NMR, GC-MS and MS data for $[BzPip]^+$, $[BTMA]^+$ and $[BzPyr]^+$ in alkaline stability studies

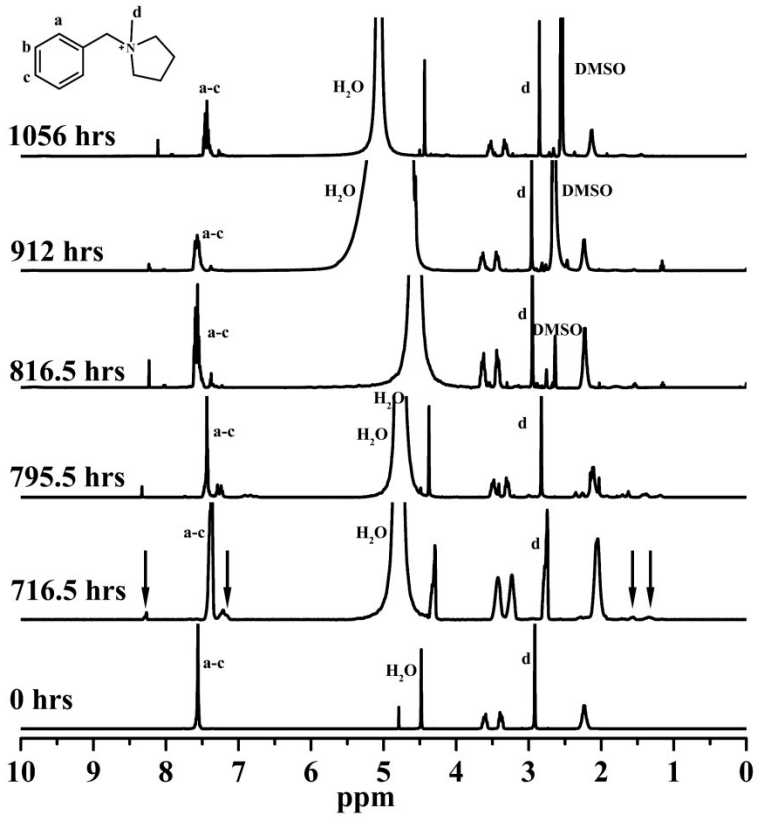

Figure S4. ^1H NMR spectra for degradation study of $[BzPyr]^+$ from 0 to 1056 h at 100 ℃ in 7 M KOH aqueous solution. The calculated extents of cation remaining are 100%, 90.4%, 74,3%, 78.3%, 74.3% and 75% for 0 h, 716.5 h, 795.5 h, 816 h, 912 h and 1056 h, respectively.

Note: the peaks pointed out by arrows correspond to new substances appearing in the test.

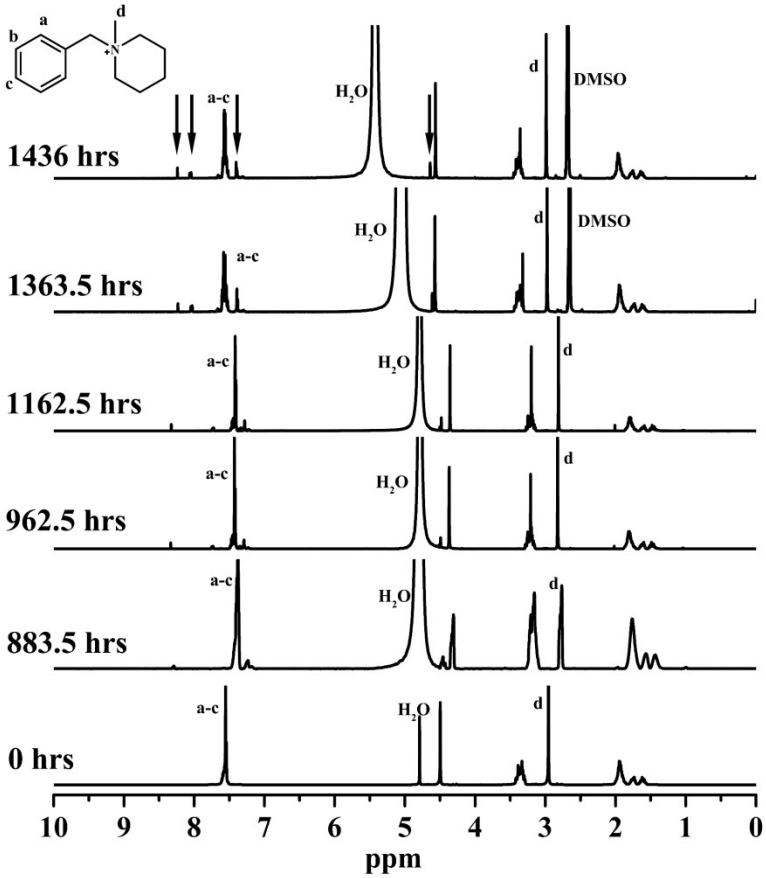

Figure S5. ^{1}H NMR spectra for degradation study of $[BzPip]^{+}$ from 0 to 1436 h at 100 ℃ in 7 M KOH aqueous solution. The calculated extents of cation remaining are 100%, 90.3%, 85.7%, 79%, 77% and 76.3% for 0 h, 883.5 h, 962.5 h, 1162.5 h, 1363.5 h and 1436 h, respectively.

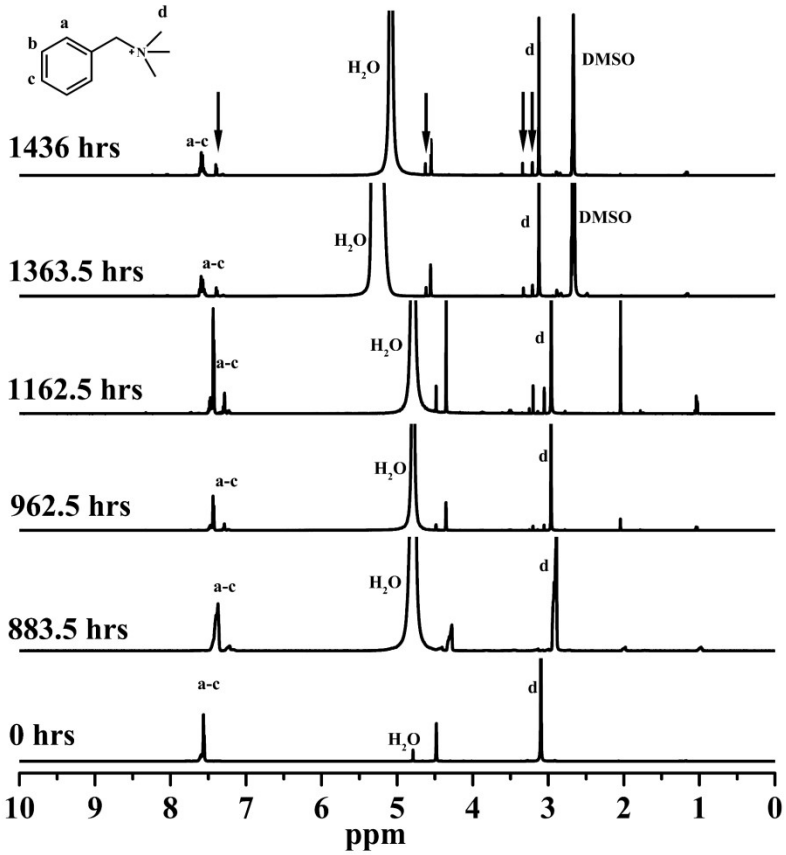

Figure S6. ^{1}H NMR spectra for degradation study of $[BTMA]^{+}$ from 0 to 1436 h at 100 ℃ in 7 M KOH aqueous solution. The calculated extents of cation remaining are 100%, 90.8%, 86.1%, 82.7%, 77% and 77.1% for 0 h, 883.5 h, 962.5 h, 1162.5 h, 1363.5 h and 1436 h, respectively.

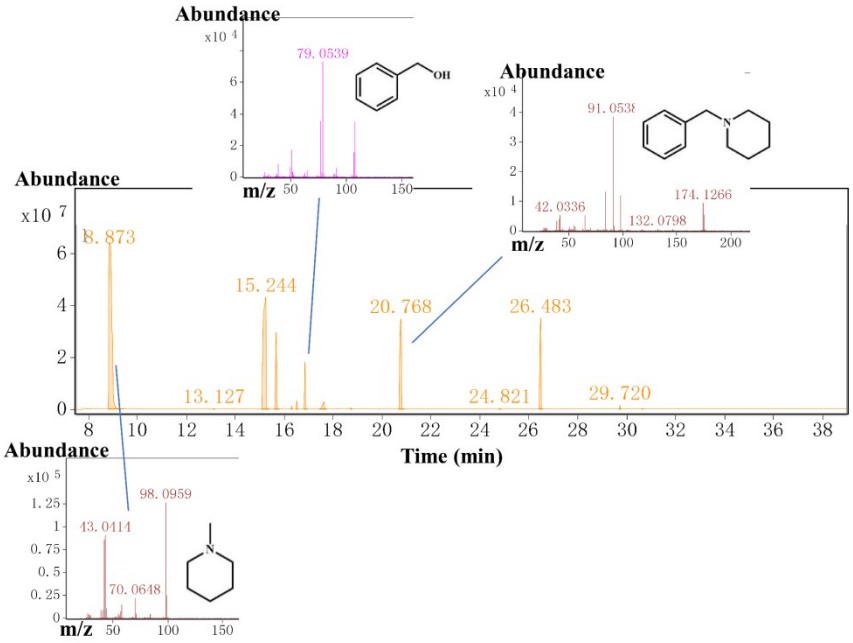

Figure S7. GC-MS analysis of $[BzPip]^+$ organic phase after 1436 h test

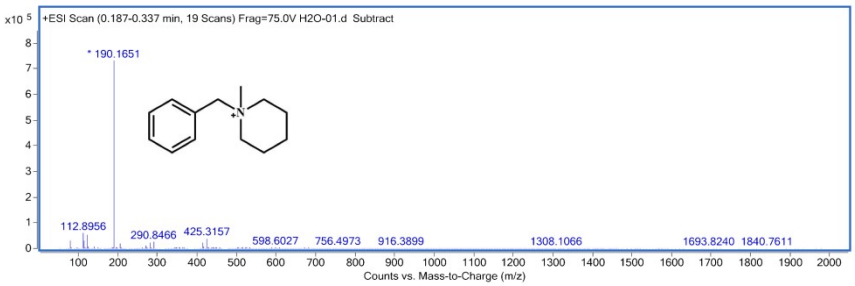

Figure S8. MS analysis of $[BzPip]^+$ aqueous phase after 1162.5 h test.

Note: The original $[BzPip]^+$ cation is found to be predominant in the aqueous phase. Besides, a strong signal appears at 8.38 ppm in the ^1H NMR spectrum. It corresponds to the aldehyde hydrogen of potassium formate, which is possibly produced from methanol (the byproduct of the S_N2 degradation route). This can be verified by the similar ^1H NMR spectrum for anhydrous methanol after being treated under the same condition.

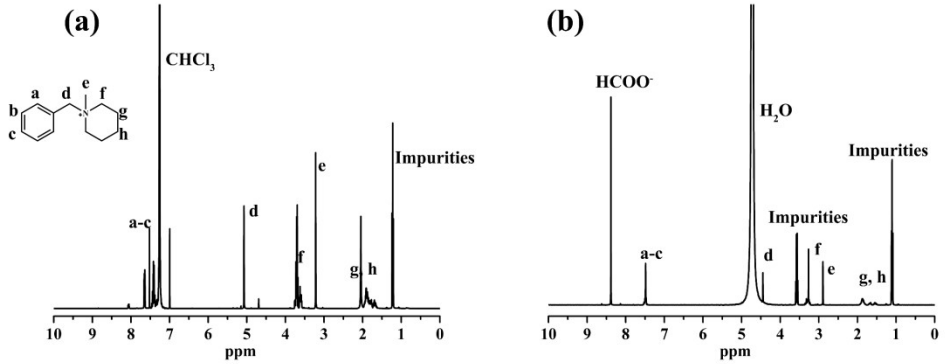

Figure S9. ^{1}H NMR spectra of $[BzPip]^{+}$ organic (a) and aqueous (b) phase after 1162.5 h test

Note: As the aqueous solution was dilute, the peaks for the impurities derived from chloroform was significant.

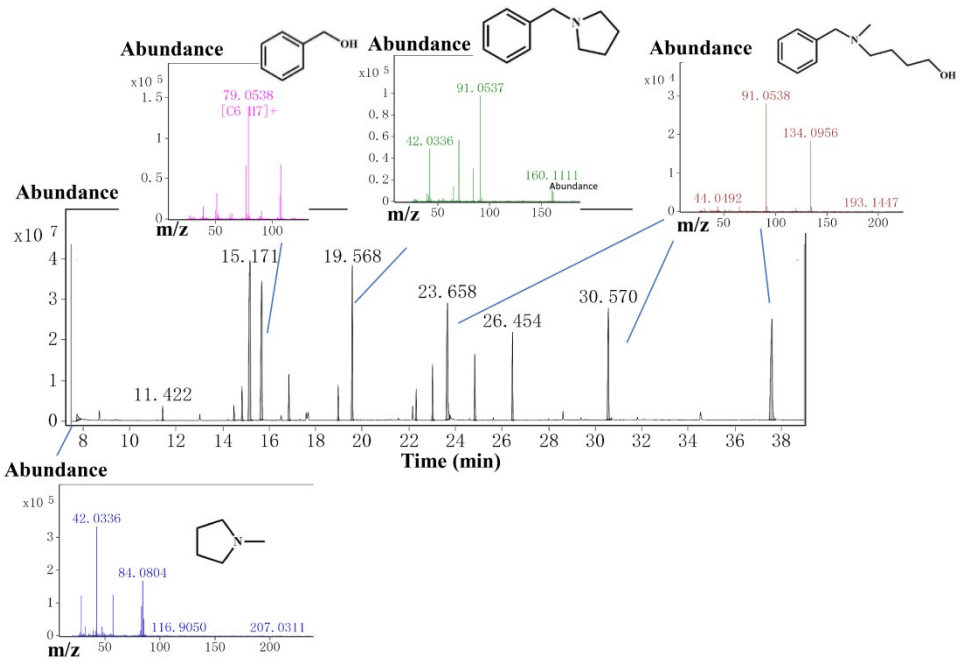

Figure S10. GC-MS analysis of $[BzPyr]^{+}$ organic phase after 1056 h test.

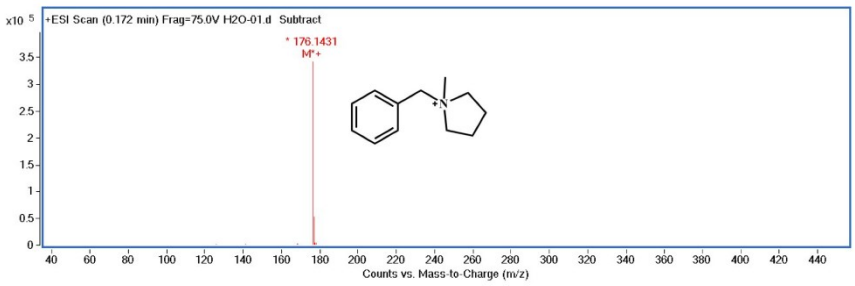

Figure S11. MS analysis of $[BzPyr]^+$ aqueous phase after 816 h test.

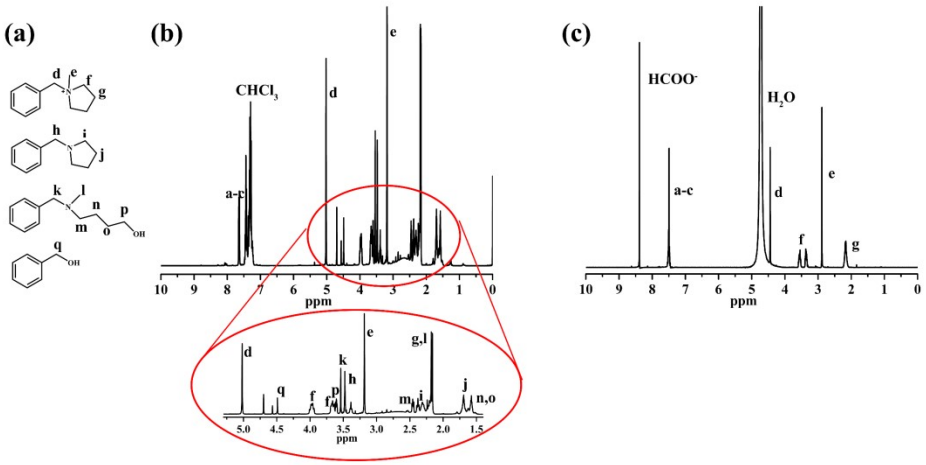

Figure S12. Suggested byproducts (a) and ^1H NMR spectra of $[BzPip]^+$ organic (b) and aqueous (c) phase after 816 h test.

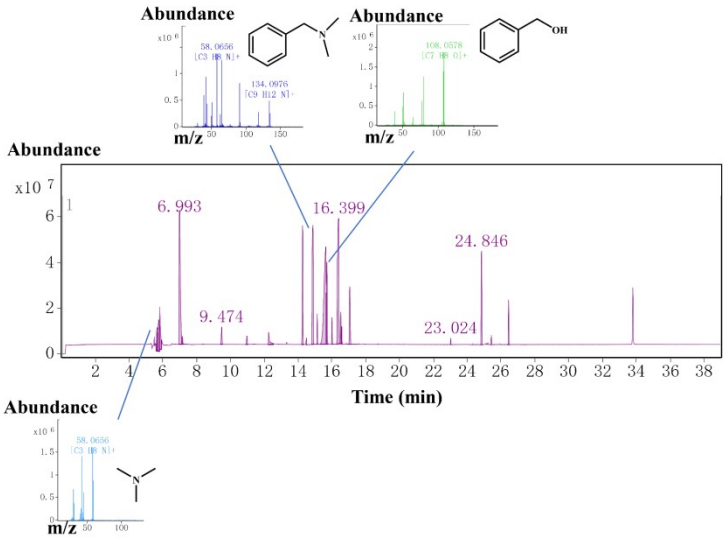

Figure S13. GC-MS analysis of $[BTMA]^+$ solution after 1436 h test.

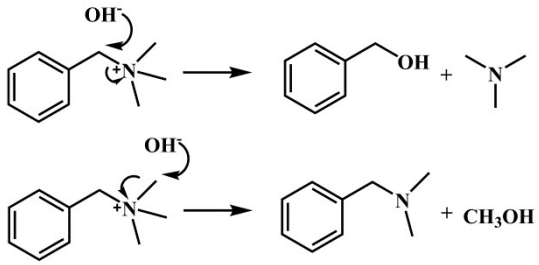

Figure S14. Potential degradation routes for $[BTMA]^+$ in 7 M KOH at 100 ℃.

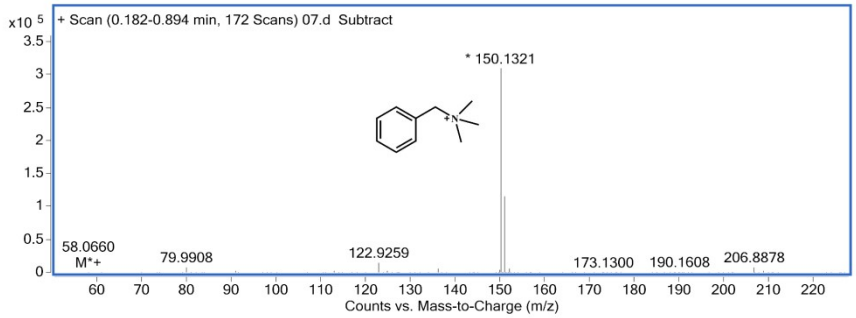

Figure S15. MS analysis of $[BTMA]^+$ solution in 7 M KOH after 1436 h test.

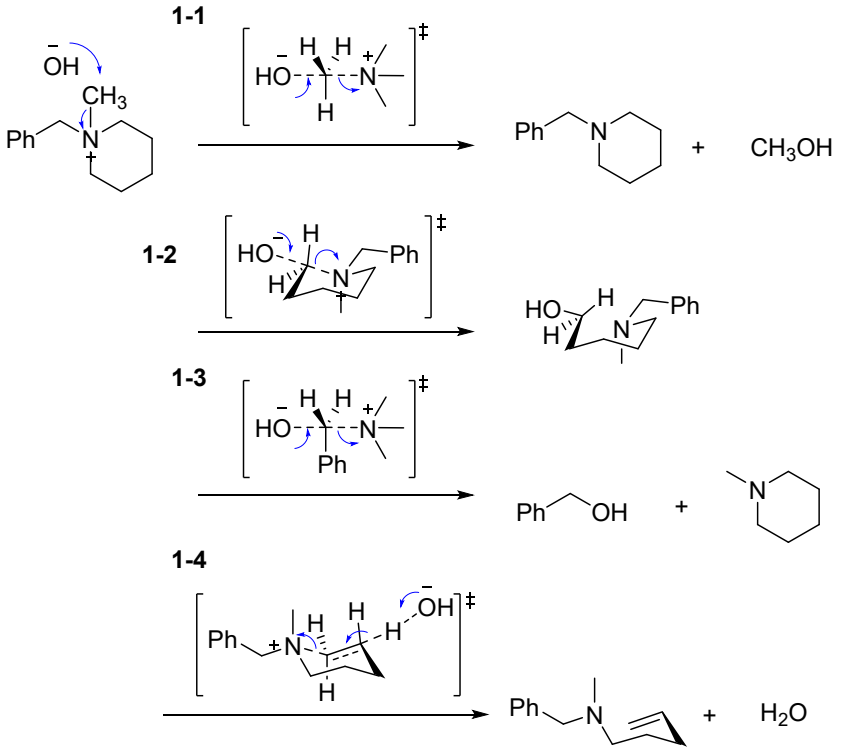

Figure S16. Proposed reaction pathways of [Bzpip]+.

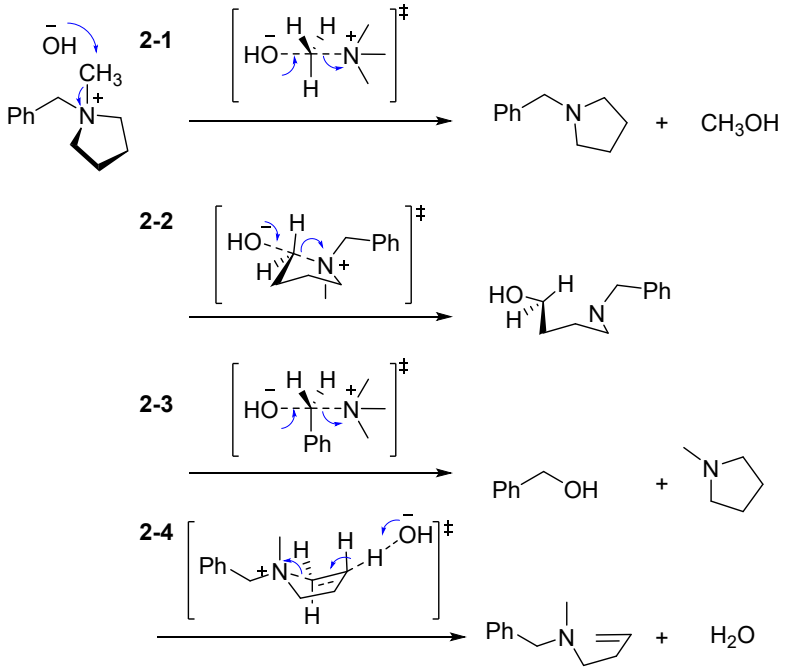

Figure S17. Proposed reaction pathways of $[Bzpyr]^+$.

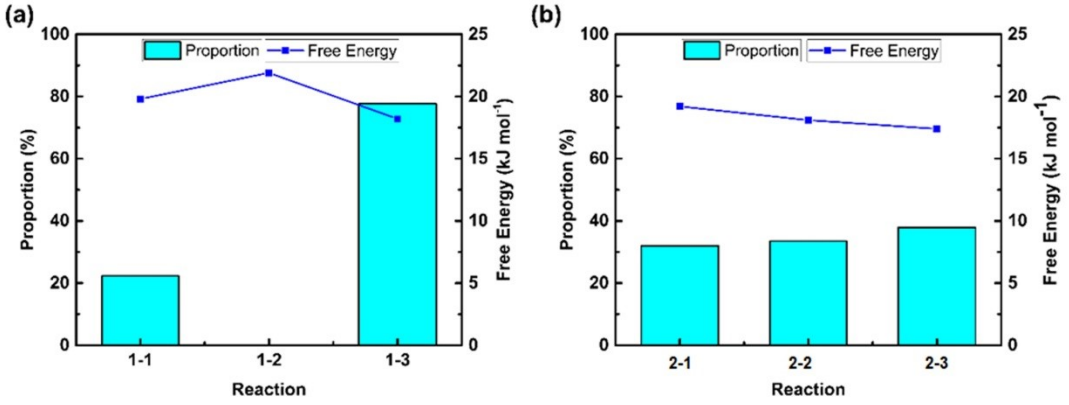

Figure S18. Free energies and proportion of each substitution reaction in Figure S16 for $[Bzpip]^+$ (a) and in Figure S17 for $[Bzpyr]^+$ (b)

Table S2. Different conformations for a certain transformation are found optimized by Gaussian 16 at B3LYP/6 6-311++G(2d,p) level with PCM solvation model (solvent=water).

Entry	ΔE (kcal/mol)	ΔG (kcal/mol)
bzpyr-R	**0.0**	***0.0***
bzpyr-TS-2-1-c1	**20.8**	***19.2***
bzpyr-TS-2-1-c2	**21.3**	***19.7***
bzpyr-TS-2-1-c3	**21.3**	***19.7***
bzpyr-TS-2-1-c4	**21.3**	***19.8***
bzpyr-TS-2-1-c5	**22.5**	***21.2***
bzpyr-TS-2-1-c6	**23.0**	***21.6***
bzpyr-TS-2-1-c7	**22.5**	***21.7***
bzpyr-P-2-1	**-20.3**	***-28.2***
bzpyr-TS-2-2-c1	**18.2**	***18.1***
bzpyr-TS-2-2-c2	**18.6**	***18.1***
bzpyr-TS-2-2-c3	**18.5**	***18.6***
bzpyr-TS-2-2-c4	**19.4**	***18.7***
bzpyr-TS-2-2-c5	**19.4**	***18.9***
bzpyr-TS-2-2-c6	**19.8**	***19.2***
bzpyr-TS-2-2-c7	**19.8**	***19.4***
bzpyr-TS-2-2-c8	**19.8**	***19.4***
bzpyr-TS-2-2-c9	**19.8**	***19.6***
bzpyr-TS-2-2-c10	**19.8**	***19.6***
bzpyr-TS-2-2-c11	**19.8**	***19.6***
bzpyr-TS-2-2-c12	**19.8**	***19.9***
bzpyr-TS-2-2-c13	**19.8**	***19.9***
bzpyr-TS-2-2-c14	**20.8**	***20.6***
bzpyr-TS-2-2-c15	**20.8**	***21.0***
bzpyr-P-2-2	**-22.6**	***-23.7***
bzpyr-TS-2-3-c1	**19.5**	***17.4***
bzpyr-TS-2-3-c2	**20.4**	***18.8***
bzpyr-TS-2-3-c3	**20.4**	***19.3***
bzpyr-TS-2-4-c1	**19.6**	***14.7***
bzpyr-P-2-3	**-23.7**	***-32.1***
bzpyr-TS-2-4-c2	**19.1**	***15.0***
bzpyr-TS-2-4-c3	**19.2**	***15.0***
bzpyr-TS-2-4-c4	**19.6**	***15.6***
bzpyr-TS-2-4-c5	**20.6**	***16.6***
bzpyr-TS-2-4-c6	**20.9**	***17.4***
bzpyr-P-2-4	**-18.4**	***-26.1***
□		
bzpip-R	**0.0**	***0.0***
bzpip-TS-1-1-c1	**21.0**	***19.8***
bzpip-TS-1-1-c2	**21.7**	***20.5***
bzpip-TS-1-1-c3	**21.8**	***20.8***

bzpip-TS-1-1-c4	**21.8**	***20.7***
bzpip-TS-1-1-c5	**21.8**	***20.8***
bzpip-P-1-1	**-22.2**	***-30.5***
bzpip-TS-1-2-c1	**22.7**	***21.9***
bzpip-TS-1-2-c2	**23.7**	***23.2***
bzpip-TS-1-2-c3	**24.1**	***23.3***
bzpip-TS-1-2-c4	**26.9**	***25.8***
bzpip-P-1-2	**-17.5**	***-19.8***
bzpip-TS-1-2-c1	**22.9**	***22.0***
bzpip-TS-1-2-c2	**23.8**	***23.1***
bzpip-TS-1-2-c3	**26.7**	***25.7***
bzpip-TS-1-3-c1	**19.2**	***18.2***
bzpip-TS-1-3-c2	**19.4**	***18.3***
bzpip-TS-1-3-c3	**19.6**	***18.7***
bzpip-P-1-3	**-25.6**	***-34.3***
bzpip-TS-1-4-c1	**19.2**	***14.7***
bzpip-TS-1-4-c2	**19.8**	***15.3***
bzpip-TS-1-4-c3	**20.5**	***16.0***
bzpip-TS-1-4-c4	**19.4**	***15.0***
bzpip-TS-1-4-c5	**19.9**	***15.5***
bzpip-TS-1-4-c6	**25.5**	***20.6***
bzpip-P-1-4	**-14.3**	***-23.5***

5. NMR spectra for cations synthesized for substituent effect studies

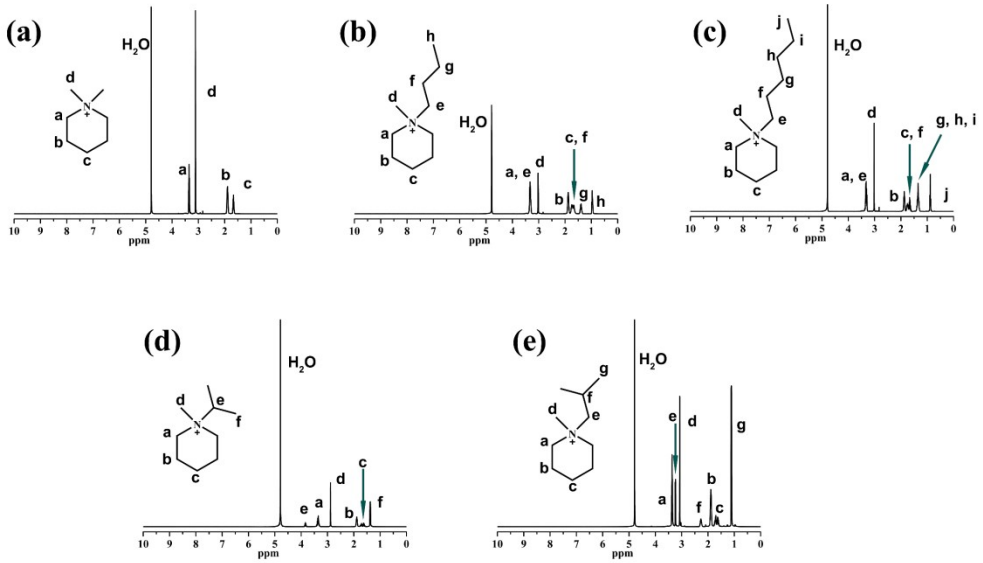

Figure S19. ^{1}H NMR spectra of $[MePip]^{+}$ (a), $[BuPip]^{+}$ (b), $[HePip]^{+}$ (c), $[iPrPip]^{+}$ (d) and $[iBuPip]^{+}$ (e) synthesized for stability study.

6. NMR, GC-MS and MS data for cations in substituent effect studies

To give better insights into the substituent effect on the degradation behavior of piperidinium cation in alkaline environment, the degradation product in the organic phase of $[HePip]^+$, $[iPrPip]^+$ and $[iBuPip]^+$ was characterized by GC-MS (Figure S22, S24 and S26), while the composition of aqueous phase was characterized by MS (Figure S23, S25 and S27). The signals of N-alkylpiperidine and N-methylpiperidine appeared in GC-MS. Therefore, these cations underwent substitution reaction on the α-C atoms in N-methyl and alkyl groups. Additionally, the severe degradation of $[iPrPip]^+$ might derive from six β-H atoms in isopropyl group, which is prone to Hofmann elimination. However, we cannot determine the occurrence of E2 elimination because the short-chain olefin byproduct was difficult to detect in the experimental condition.

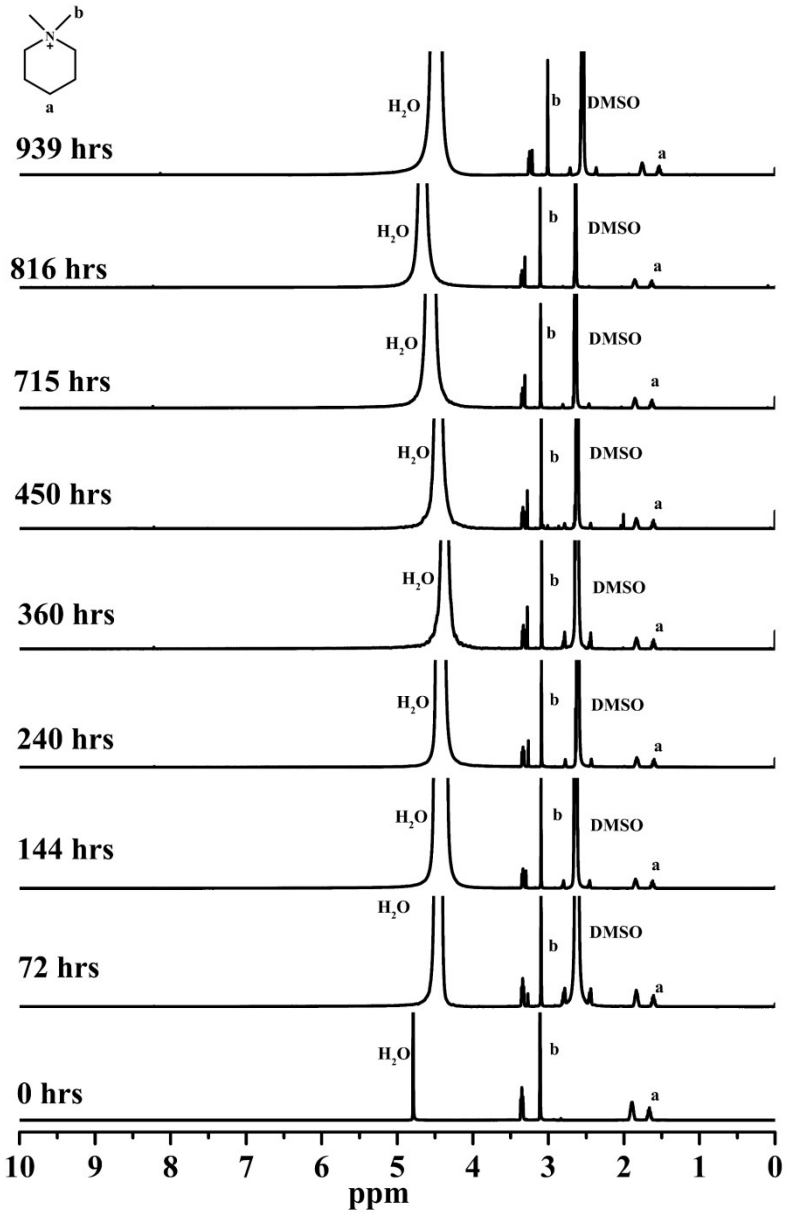

Figure S20. ^{1}H NMR spectra for degradation study of $[MePip]^{+}$ from 0 to 939 h at 100 ℃ in 7 M KOH aqueous solution. No obvious degradation was detected during the test.

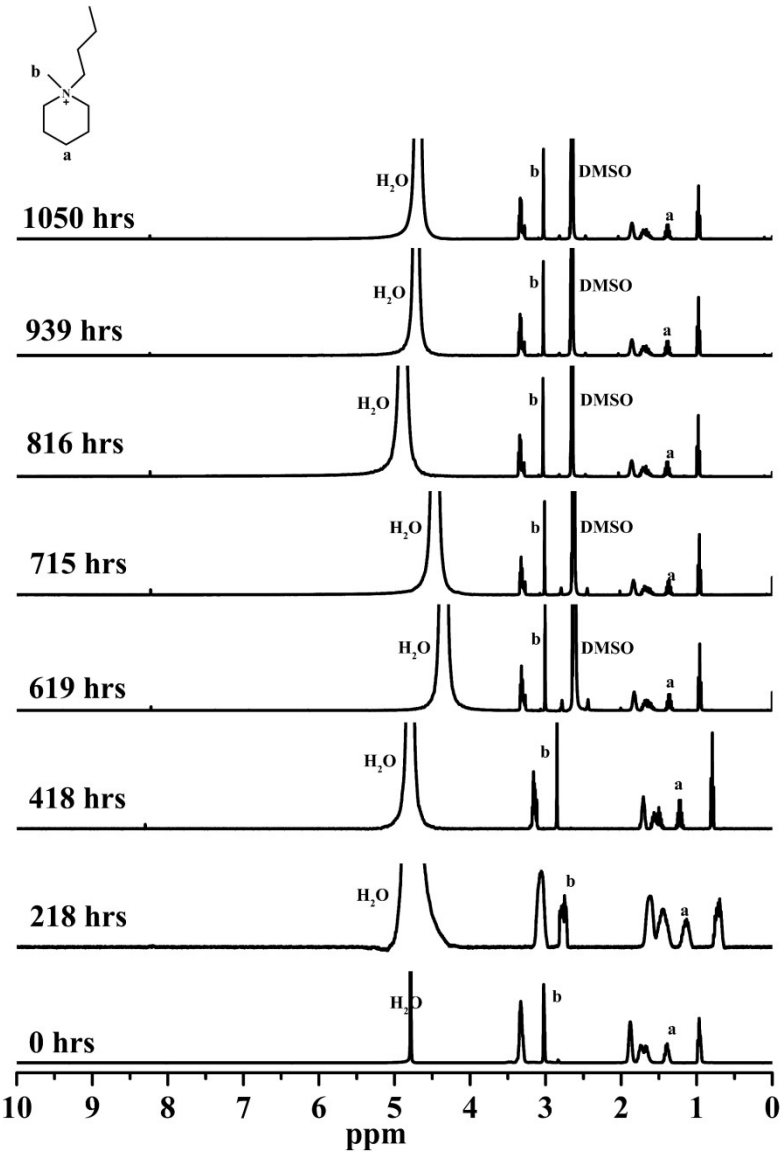

Figure S21. ^{1}H NMR spectra for degradation study of $[BuPip]^{+}$ from 0 to 1050 h at 100 ℃ in 7 M KOH aqueous solution. No obvious degradation was detected during the test.

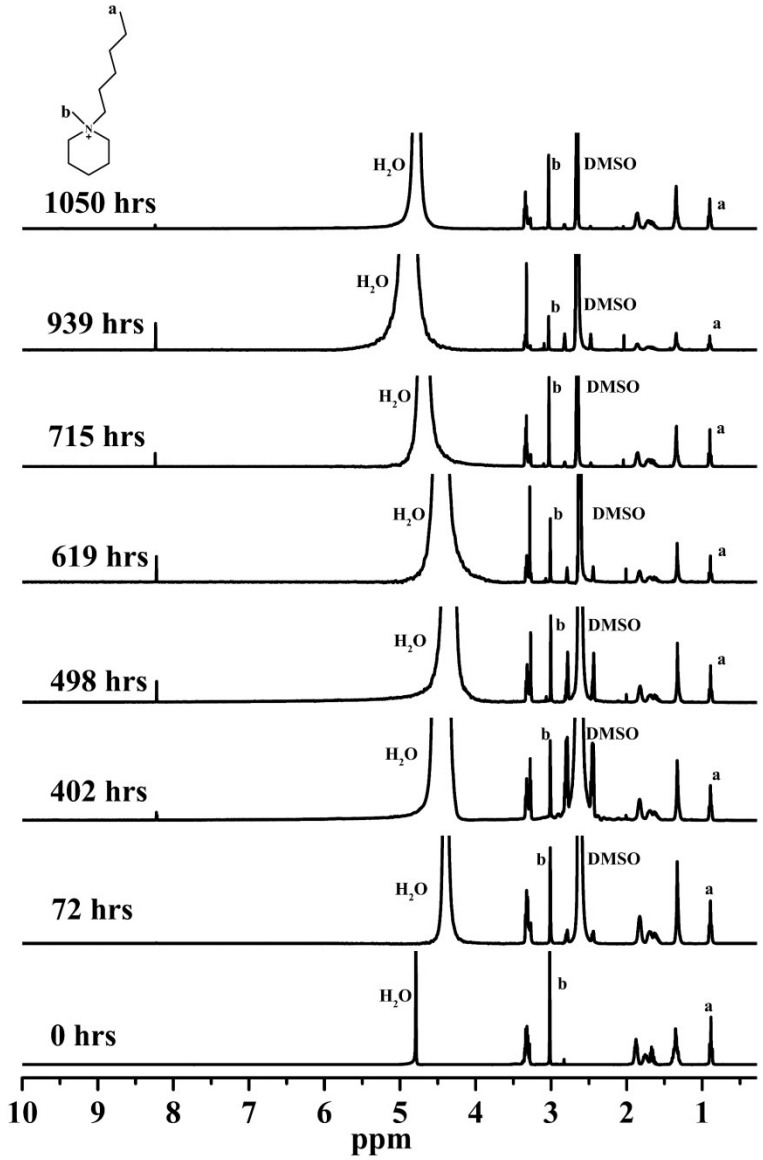

Figure S22. ^{1}H NMR spectra for degradation study of $[HePip]^{+}$ from 0 to 1050 h at 100 ℃ in 7 M KOH aqueous solution. The calculated extents of cation remaining are 100% from 0 h to 498 h test and 93%, 93.7%, 85% and 73.3% for 570 h, 619 h, 715 h, 939 h, 1050 h, respectively.

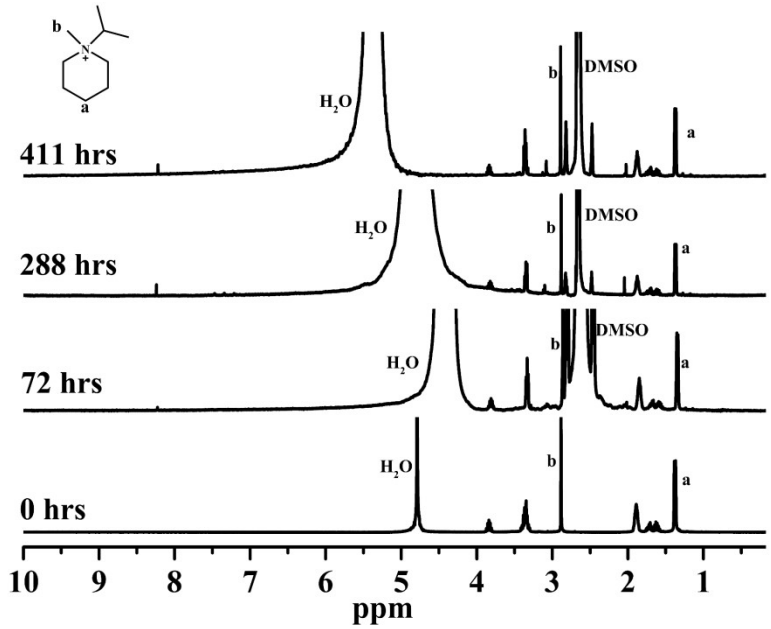

Figure S23. ^{1}H NMR spectra for degradation study of $[iPrPip]^{+}$ from 0 to 411 h at 100 ℃ in 7 M KOH aqueous solution. The calculated extents of cation remaining are 100%, 88%, 77%, and 84% for 0 h, 72 h, 288 h and 411 h, respectively.

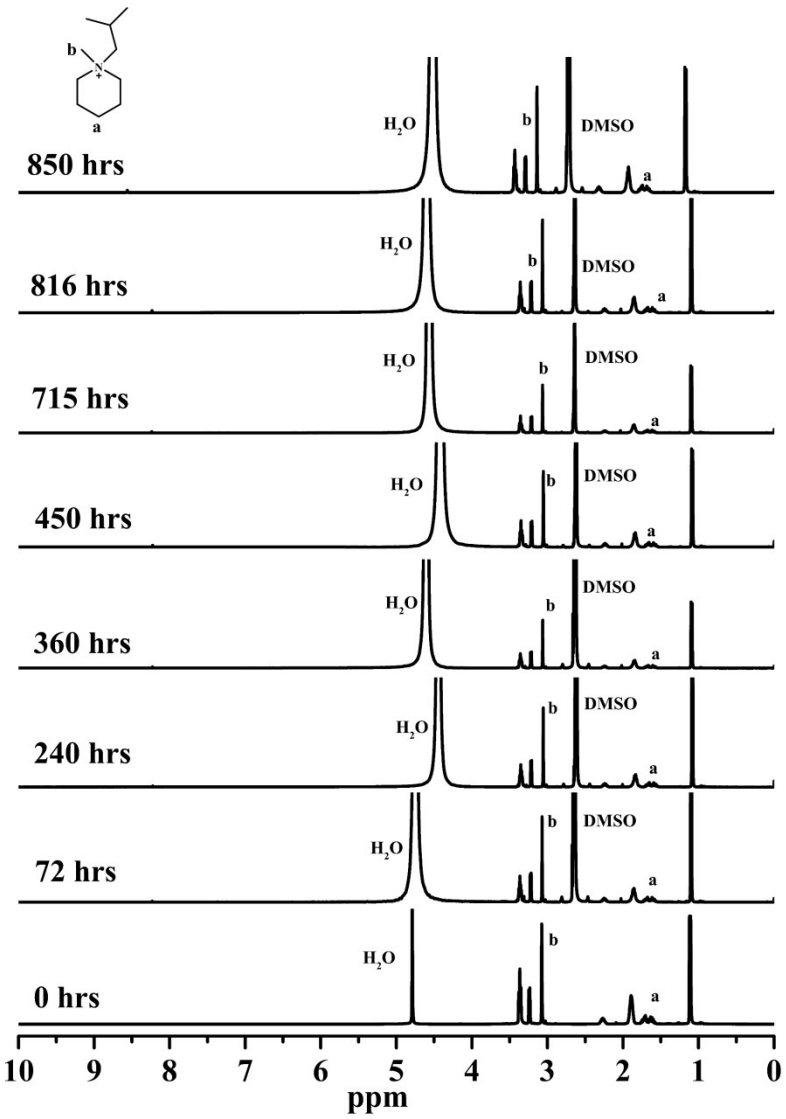

Figure S24. ^{1}H NMR spectra for degradation study of [iBuPip]$^{+}$ from 0 to 850 h at 100 ℃ in 7 M KOH aqueous solution. The calculated extents of cation remaining are 100%, 92%, 94.7%, 98%,100% 90%, 93.35% and 94.3% for 0 h, 72 h, 240 h, 360 h, 450 h, 715 h, 816 h and 850 h, respectively.

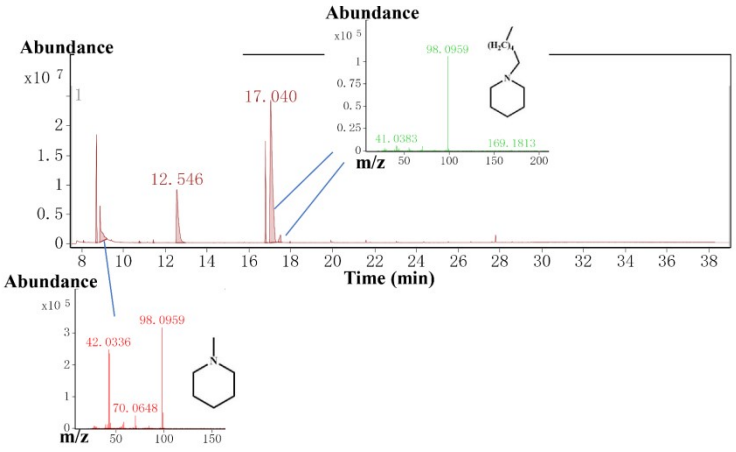

Figure S25. GC-MS analysis of $[HePip]^+$ organic phase after 1050 h test.

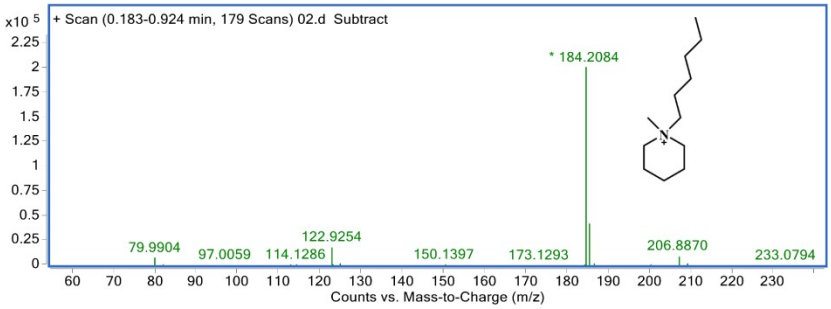

Figure S26. MS analysis of $[HePip]^+$ aqueous phase after 1050 h test.

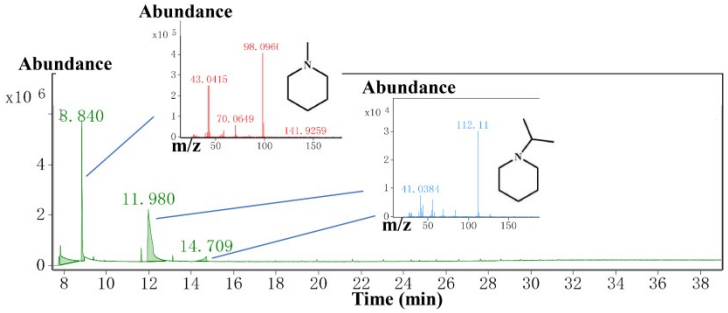

Figure S27. GC-MS analysis of $[iPrPip]^+$ organic phase after 411 h test.

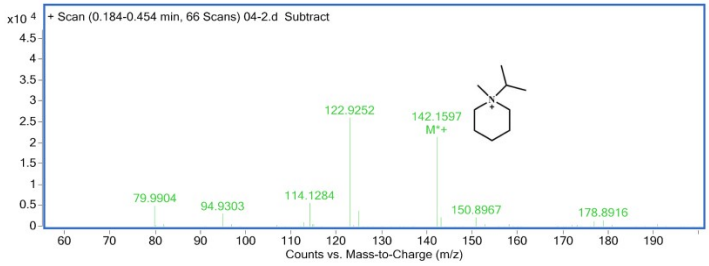

Figure S28. MS analysis of $[iPrPip]^+$ aqueous phase after 411 h test.

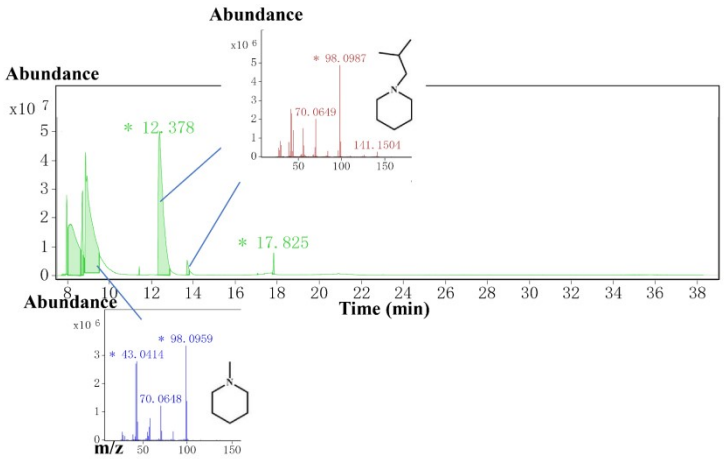

Figure S29. GC-MS analysis of $[iBuPip]^+$ organic phase after 850 h test.

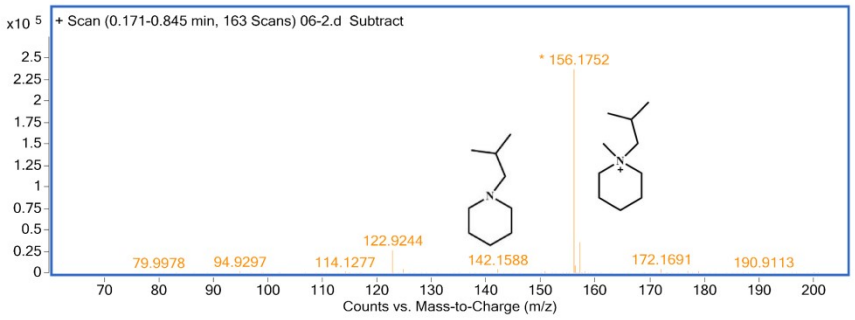

Figure S30. MS analysis of $[iBuPip]^+$ aqueous phase after 850 h test.

7. The degradation extent of cations in this work and comparison with literature.

Table S3. Comparison of chemical stability for cations in Figure 6.

Cation	Alkali concentration	Temperature	Time	Cation remaining	Ref.
	(M)	(℃)	(h)	(%)	
$[BuPip]^+$	7	100	1050	100	This work
$[MePip]^+$	7	100	939	100	This work
$[HePip]^+$	7	100	1050	93.3	This work
$[iBuPip]^+$	7	100	850	94.3	This work
$[iPrPip]^+$	7	100	411	84	This work
$[BzPip]^+$	7	100	883.5	90.3	This work
$[BTMA]^+$	7	100	883.5	90.8	This work
$[BzPyr]^+$	7	100	795.5	75	This work
DPPipQ	2	120	366	100	[1]
DMP	6	160	87.3	50	[2]
BMP	6	160	7.3	50	[2]
$[HePip]^+$	2	80	720	94	[3]
$[EMPy]^+$	1	80	168	96.78	[4]
QDM	1	60	72	54	[5]

REFERENCES

1 Olsson JS, Pham TH, Jannasch P. Poly(arylene piperidinium) hydroxide ion exchange membranes: Synthesis, alkaline stability, and conductivity. *Advanced Functional Materials*, 2018, 28(2): 1702758

2 Marino MG, Kreuer KD. Alkaline stability of quaternary ammonium cations for alkaline fuel cell membranes and ionic liquids. *ChemSusChem*, 2015, 8(3): 513-523

3 You W, Ganley JM, Ernst BG, et al. Expeditious synthesis of aromatic-free piperidinium-functionalized polyethylene as alkaline anion exchange membranes. *Chem Sci*, 2021, 12(11): 3898-3910

4 Gu F, Dong H, Li Y, et al. Base stable pyrrolidinium cations for alkaline anion exchange membrane applications. *Macromolecules*, 2014, 47(19): 6740-6747

5 Wang B, Sun W, Bu F, et al. Comparison of alkaline stability of benzyltrimethylammonium, benzylmethylimidazolium and benzyldimethylimidazolium functionalized poly(arylene ether ketone) anion exchange membranes. *International Journal of Hydrogen Energy*, 2016, 41(4): 3102-3112